Available online at www.sciencedirect.com

ScienceDirect

Energy Procedia 49 (2014) 694 – 704

Energy Procedia

SolarPACES 2013

Comparison of thermocline molten salt storage performances to commercial two-tank configuration

G. Angelini, A. Lucchini, G. Manzolini *

Department of Energy, Politecnico di Milano, via Lambruschini 4, 20156, Milano (Italy)
** Corresponding author tel:+39 02 2399 2810, e-mail: giampaolo.manzolini@polimi.it*

Abstract

This work deals with the assessment of thermocline heat storage performances when applied to solar thermal plants. The considered thermocline is based on molten salt heat transfer fluid (Solar Salts between 300°C and 550°C) and filled with quartzite. A 2-D finite element heat transfer model is developed to determine the temperatures inside the vessel with mass flows input/output. The model includes heat conductivity of molten salt and quartzite rocks, heat transfer between the molten salts and the quartzite, as well as heat loss to the environment. Results of the model are compared to available experimental data as well as analytic results showing good agreement. Then, the thermocline storage with the performances predicted by the 2-D code was integrated in a CSP plant previously modelled with the two-tank TES system. Plant management is kept equal to the two-tank configuration. A performance index is introduced to make a consistent comparison between the thermocline and the two-tank system: storage efficiency is defined as the heat withdrawn from the storage above 545°C divided by the overall input in the storage. The defined index is equal to 100% for the two tank system as thermal losses have a negligible impact. On the contrary, in thermocline storage, part of heat stored in the molten salt is in the thermocline region and this molten salt is not accounted as useful. The thickness of the thermocline is about 4 to 6 meter height out of 14 meters making the storage performances in the range of 65%, hence significantly lower than in two-tank configuration. A sensitivity analysis on tank size and tank shape factor is performed to assess the optimal configuration for the thermocline.

Selection and peer review by the scientific conference committee of SolarPACES 2013 under responsibility of PSE AG.
Final manuscript published as received without editorial corrections.

Keywords: Solar Thermal Energy; Thermal Energy Storage; Thermocline; Molten Salt

1. Introduction

The research in the exploitation of renewable resources can be the answer to the issues related to greenhouse gases. Concentrated solar power (CSP) is a promising technology which exploits solar radiation to supply

1876-6102
Selection and peer review by the scientific conference committee of SolarPACES 2013 under responsibility of PSE AG.
Final manuscript published as received without editorial corrections.
doi:10.1016/j.egypro.2014.03.075

electricity. An interesting feature of those plants is the thermal energy storage (TES) which allows producing electricity decoupled from the solar availability. Since the thermal energy storage is responsible of about 20% of the cost of the entire CSP plant, a cost reduction would be advantageous making larger storages convenient, with benefits electricity cost wise [1]. Between the possible TES configurations, direct storage of molten salt in thermocline vessels is characterized by lower investment cost than state-of-art two-tank systems (for example, the two-tank systems of Andasol, SEGS I and Gemasolar CSP plants) [1] [2] [3] [4]. Molten salt thermocline TES systems are less expensive for two reasons. First, the number of storage vessels is reduced. Second, the vessel is filled with a low-cost packed bed, which acts as primary thermal energy storage. It has been assessed that the thermocline has an investment cost up to 33% lower than a two-tank system with the same energy capacity [2].

Unfortunately, thermocline TES system is characterized by lower discharge efficiency than the two-tank system. In the vessel, hot and cold molten salt are in contact and a thermal gradient is present along the axis of the tank; this thermal gradient is called "thermocline" (Figure 1). If the thermocline had infinitesimal thickness, thermal stratification would be perfect.

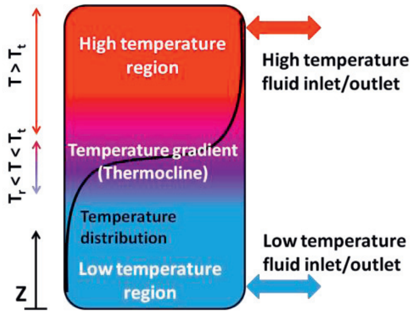

Figure 1: Sketch of thermocline thermal energy storage

Nomenclature

c_p	specific heat capacity, J kg^{-1} K^{-1}
D	vessel diameter, m
D_{pb}	average packed bed rock diameter, m
H	vessel height, m
h	heat transfer coefficient, W m^{-2} K^{-1}
h_v	volumetric heat transfer coefficient,Wm^{-3} K^{-1}
k	thermal conductivity, W m^{-1} K^{-1}
Pe	Péclet number
Pr	Prandtl number
r	radius, m
Re	Reynolds number
t	time, s
t_{charge}	time at which the vessel is being charged, s
$t_{discharge}$	time at which the vessel is being charged, s
T	temperature, K
T_n	nominal temperature, K
T_r	reference temperature, K
T_t	threshold temperature, K
T_H	temperature at the top port of the vessel, K
T_L	temperature at the bottom port of the vessel, K
u_m	velocity before the packed bed, m s^{-1}
u	velocity, m s^{-1}
z	location along the axis of the tank, m
z_t	z at which $T=T_t$, m

Greek

ε	porosity in the packed bed region
η	efficiency
μ	viscosity, kg m^{-1} s^{-1}
ρ	density, kg m^{-3}

Subscripts

eff	effective
ms	molten salt
pb	solid filler, packed bed
ss	Solar Salt
sto	stored
with	withdrawn

Acronyms

CSP	concentrated solar power
HTF	heat transfer fluid
TES	thermal energy storage

In this work, molten salt temperature ranges between 300°C and 550°C and molten salt at 550°C coming from the solar field is directly stored at the top of the thermocline (direct storage). When collected heat at the solar field is not sufficient to drive the power block, molten salt is withdrawn from the top of the tank. The temperature at the output port of the thermocline is steadily 550°C until the thermal gradient reaches the top of the tank. At this point, the output temperature starts to drop. On the other hand, the output temperature of two-tank storages is steadily 550°C. The aim of the present work is the assessment of the performance of thermocline TES system together with the research on some parameters which may affect its storage efficiency.

2. Model development

2.1. Hypothesis

A finite-difference numerical model is developed to predict the performance of the thermocline. Assumptions made are:

The filler is assumed to be isotropic, homogenous and continuous. The physical properties of the packed bed are assumed to be constant (see Table 1), while those of the molten salt are temperature dependent. The chosen molten salt is Solar Salt with properties taken from [5]. This correlation are valid in the studied temperature range (T in °C):

Density [kg/m3]	$\rho_{ss} = 2090 - 0{,}636 \cdot T$
Heat capacity [J/kgK]	$c_{p_{ss}} = 1443{,}2 - 0{,}172 \cdot T$
Viscosity [$mPa \cdot s$]	$\mu_{ss} = 22{,}714 - 0{,}12\,T + 2{,}281 \cdot 10^{-4}\,T^2 - 1{,}474 \cdot 10^{-7}\,T^3$
Thermal conductivity [W/mK]	$k_{ss} = 0{,}443 + 1{,}9 \cdot 10^{-4} \cdot T$

- Viscous effects and vortex are considered as secondary and negligible [5].
- Molten salt flow through the packed bed is one-dimensional, laminar and aligned with the tank axis [5]. Hence, no radial velocity is considered.
- The heat transfer problem is considered to be 2D, axisymmetric.
- Thermal diffusion is accounted only in the molten salt energy equation by an effective thermal conductivity: this coefficient is a combination of the thermal conductivity of the molten salt and of the thermal conductivity of the packed bed.

2.2. Fundamental equations

The numerical model is developed from three fundamental equations. Schumann equations (eq. (1)(2)- (3)), which accounts for energy yield of the molten salt and the packed bed [6], and mass conservation (eq.(1)). Molten salt velocity is defined as in eq. (4).

$$\begin{cases} \varepsilon \dfrac{\partial \rho_{ms}}{\partial t} + div(\rho_{ms} u_m) = 0 & (1) \\ \varepsilon \rho_{ms} c_{p,ms} \dfrac{\partial T_{ms}}{\partial t} + \rho_{ms} c_{p,ms} u_m \dfrac{\partial \mathrm{T_{ms}}}{\partial z} = \dfrac{\partial}{\partial z}\left(k_{eff} \dfrac{\partial T_{ms}}{\partial z}\right) + \dfrac{1}{r}\dfrac{\partial}{\partial r}\left(k_{eff} r \dfrac{\partial T_{ms}}{\partial r}\right) + h_v\left(T_{pb} - T_{ms}\right) & (2) \\ (1-\varepsilon)\rho_{pb} c_{p,pb} \dfrac{\partial T_{pb}}{\partial t} = h_v\left(T_{ms} - T_{pb}\right) & (3) \end{cases}$$

$$u_m = \varepsilon \cdot u \quad (4)$$

k_{eff} is the effective thermal conductivity of the molten salt and the packed bed, exponential averaged, [5]:

$$k_{eff} = k_{ms}^{\varepsilon} + k_{pb}^{1-\varepsilon} \quad (5)$$

h_v is the volumetric heat transfer coefficient. Xu et al [5] compare several relationships for the evaluation of h_v. According to their research, the following formula is chosen (eq. (6)) [5] [7]. This equation has no particular Reynolds or Prandtl numbers limitation.

$$h_v = 6 \cdot \left(2 + 1{,}1 * Pr_{ms}^{\frac{1}{3}} \cdot Re_d^{0.6}\right) \cdot \frac{k_{ms}}{D_{pb}} \cdot \frac{1-\varepsilon}{D_{pb}} \quad (6)$$

For the detail on these correlations, it can be referred to books such as “Heat transfer in packed beds” [8] or the paper of Xu [5].

2.3. Boundary conditions and discretization

The boundary conditions imposed are:

- $\left.\frac{\partial T}{\partial r}\right|_{r=0} = 0$ at the center of the tank, because of symmetry considerations,
- $\left.\frac{\partial T}{\partial r}\right|_{r=R} = \left(h_{free} + h_{forced}\right)\left(T - T_{inf}\right) + \varepsilon\sigma(T^4 - T_i^4)$: free and forced convection plus radiation to the environment,
- $u(z = H) = u(t)$: axial velocity (and hence, mass flow rate charged/discharged) imposed at the top port,
- $\left.\frac{\partial T}{\partial z}\right|_{z=0,z=H} = 0$: the top and the bottom of the tank are adiabatic.

In the energy yield equation of molten salt, time is discretized with an implicit downwind-differencing scheme, thermal diffusion with a centred-differencing scheme and advection with an upwind-differencing scheme. In the energy yield equation of the packed bed, time is discretized with an implicit-differencing scheme. For mass conservation equation, an implicit-differencing scheme is applied for time, and an upwind-differencing scheme for space. The model is implemented in Matlab and simulations are run until residuals become lower than 10^{-5}. A time step length of 10s, 400 axial nodes and 10 radial nodes are used for the simulations. These time step length and mesh dimension guarantee that the solution is not mesh dependent.

2.4. Experimental validation

The numerical model is compared to the experimental data published by Pacheco [2]. Also, the model is compared to the numerical model previously developed by Garimella; the same storage specifications, molten salt flow rate and environmental characteristics are assumed [10].

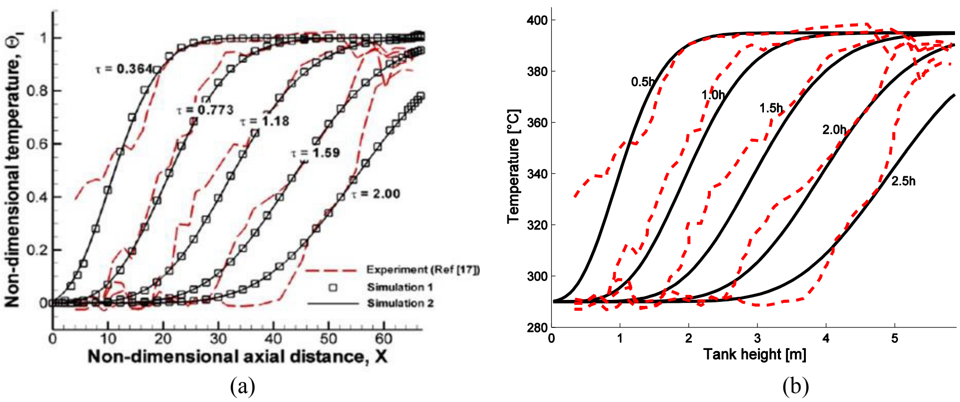

Figure 2: (a) Pacheco experimental data [2] (dashed red lines) compared to Garimella's model [10] (solid black lines); (b) Pacheco experimental data [2] (dashed red lines) and the new developed model (solid black lines)

Estimated temperature distribution (Figure 2-b) well accords with both Garimella's model (Figure 2-a) and Pacheco's data (dashed lines) (Figure 2-b) [10] validating the numerical model developed in this work.

3. Results

3.1. Definition of efficiency indicators

Real data of a CSP plant of 50 MW power output with molten salt as both the heat transfer fluid and storage medium featuring Andasol plant are assumed [11]. TES storage was managed in order (i) to limit the number of start-up/shut-down of the power plant, hence compacting the operating hours and (ii) to produce the electricity during the day when the demand from the grid is higher. Therefore, the storage is not emptied during night time, but part of the energy is used in the first hours of the morning.
The two-tank TES of this CSP plant is replaced with a thermocline with the same thermal capacity, keeping the same management. To properly compare the two energy storing technologies it is necessary to define:

1. A reference temperature: for the sake of simplicity it was chosen the lower value of the temperature range of the molten salt (T_r=300°C).
2. A threshold temperature which clearly identifies the high temperature region in the storage ($z_t < z < H$, where z_t is the level of the tank where $T=T_t$) and the thermocline region in the tank: it was chosen T_t=545°C, which is a technically acceptable approximation of the nominal operating temperature.
3. Molten salt mass flow rate withdrawn from the tank is considered as positive, while the molten salt mass flow rate stored in the vessel is assumed as negative (sign convention).
4. Discharge efficiency and collection efficiency were selected as indicators to make a consistent comparison between the thermocline and the reference two-tank system.

Part of the salt stored in the thermocline is at an average temperature between the maximum and the minimum, which differs from the two-tank systems, where molten salt are steadily withdrawn at nominal temperature. To make a consistent comparison with the two-tank system, salt withdrawn at a temperature below the threshold temperature is not accounted as "useful".

The discharge efficiency is defined as the ratio of the "useful" heat provided to the power block and the total amount of heat available (see eq. (7)). As useful, it is assumed the heat extracted from the molten salts with a temperature above the threshold temperature ($T_r < T_H < T_n$) to the reference temperature of 300°C. The Heaviside function $H(T_H-T_t)$ is added to neglect the heat from salt withdrawn at a temperature below the threshold temperature T_t. The denominator is the total heat extracted from the molten salts from the beginning (0) to the end of the simulated period (t_{end}). In this work, the evaluated period of time is a week. Since the integration has to be performed only when the tank is being discharged, the Heaviside function $H(\dot{m}_{ss})$ is added and only positive mass flow rates (i.e. the withdrawn molten salt) are effectively integrated.

$$\eta_{disch} = \frac{\int_0^{t_{end}} \dot{m}_{ss}\, c\, (T_H(t) - T_r) \cdot [H(\dot{m}_{ss})\, H(T_H - T_t)]\, dt}{\int_0^{t_{end}} \dot{m}_{ss}\, c\, (T_H(t) - T_r) \cdot [H(\dot{m}_{ss})]\, dt} \quad (7)$$

It is observed that discharge efficiency is closely related to the extension of the thermal gradient within the vessel.

Collection efficiency is defined, in a similar manner, as the heat effectively stored in the vessel on the total thermal energy collectable at the solar field (eq. (8)). The presence of the thermocline can lead to a higher temperature at the solar field inlet: when the thermal gradient (the thermocline) reaches the bottom of the vessel, solar salts are extracted at higher temperature from the tank, leading to partial defocusing of concentrators at the solar field, with consequent penalties. Since the integration has to be performed only when the thermocline is being charged, the Heaviside function $H(-\dot{m}_{ss})$ is added and only negative molten salt mass flow rates (i.e. the stored molten salt) are effectively integrated.

$$\eta_{coll} = 1 - \frac{\int_0^{t_{end}} |\dot{m}_{ss}|\ c\ (T_L(t) - T_r)\ H(-\dot{m}_{ss})\ dt}{\int_0^{t_{end}} |\dot{m}_{ss}|\ c\ (T_n - T_r)\ H(-\dot{m}_{ss})\ dt} \quad (8)$$

If the temperature T_L at the bottom port was steadily 300°C, all molten salt would be effectively stored; indeed, numerator of eq. (8) would be null and collection efficiency would be 100%.
The product of collection efficiency and discharge efficiency (eq. (9)) represents the overall storage efficiency.

$$\eta_{sto} = \eta_{coll} * \eta_{disch} = \frac{\int_0^{t_{end}} \dot{m}_{ss}\ c\ (T_H(t) - T_r)\ \cdot [H(\dot{m}_{ss})\ H(T_H - T_t)]\ dt}{\int_0^{t_{end}} |\dot{m}_{ss}|\ c\ (T_n - T_r)\ H(-\dot{m}_{ss})\ dt} \quad (9)$$

Discharge efficiency and collection efficiency are always equal to 100% for two-tank systems, while they are always below 100% for the thermocline storage.

3.2. Replacement of the two-tank storage with a similarly sized thermocline

Simulation is run on one week: 9^{th} – 15^{th} July. At first, the 7.5h two-tank TES system is replaced by thermocline storage of the same energy capacity. Main assumptions of the simulation are presented in Table 1.

Table 1: Assumptions

Thermocline tank assumptions	
Molten salt and filler	Solar Salt; Quartzite rock + silica sand
Physical properties	Molten salt: temperature dependent; Filler: Constant (ρ=2500kg/m^3, c_p=830 J/kgK [10])
Molten salt temperature range	300 °C – 550 °C
Full-load capacity	7.5 h
Tank height and diameter	14 m x 23,7 m
Wall structure	0,3 m of firebricks (k = 0,2 W/mK); 0,04 m of stainless steel (k = 20 W/mK); 0,15 m of mineral wool (k = 1 W/mK)
Other assumptions	
Temperature of external environment	25 °C
Week	09^{th} -15^{th} July
T threshold	545°C
P_{gross} of the power block	50 MW

Concerning initial thermocline conditions, an initial arbitrarily temperature is set in the tank. Afterwards, simulations are performed for 3-5 days until temperature stabilize and become cyclic. At this point, simulation on the desired week is run (9^{th} – 15^{th} July). Energy balances of the solar plants are presented in Figure 3. The weather is sunny the whole week, but on the afternoon of 13^{th} July and on 15^{th} July when some clouds partially cross the sky.

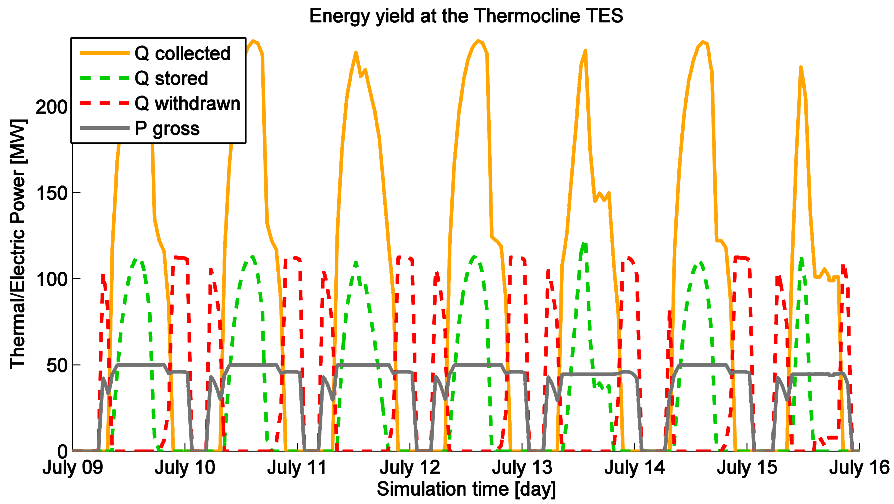

Figure 3: Energy yield on 09th – 15th July

Temperature profiles of the thermocline storage are presented for a typical day: 10th July (Figure 4-a). At 00:01, the power block is on and molten salt are withdrawn (Figure 4-b). At 1:30, the power block is turned off and withdrawing is stopped; molten salt at the top of the tank is still above the threshold temperature of 545°C. The plant remains switched off until 4:30 with a slight expansion of the thermal gradient region. At 4:30, molten salt is again withdrawn to warm up and switch on the power block. Withdrawing continues until 8:30, when solar radiation becomes enough intense to drive the power block at nominal power. During this period, the output temperature has dropped down to about 450°C. This has negative effect on power block management as well as efficiency. From 8:30 to 18:30, extra thermal power is available at the solar field and it is stored in the tank. At 18:30, the tank is almost fully charged of hot molten salt and the temperature at the bottom port of the vessel is as high as 370°C. In this case some mirrors of the solar field are placed in stowed position to avoid overheating of the solar field and some available radiation is not collected: collection efficiency drops. During night-time, withdrawing of energy continues beyond 24:00.

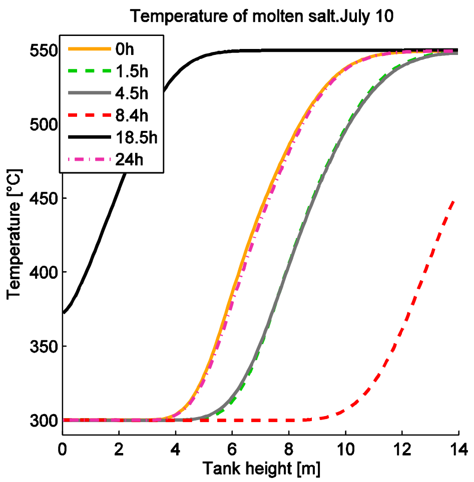

(a)

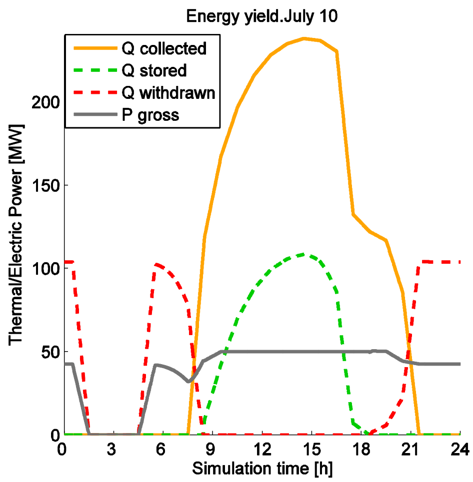

(b)

Figure 4. (a) Temperature distribution on 10th July in the thermocline at several moments of the day (b) energy yield on 10th July.

These results show that the optimal configuration for the two tank storage is different from the thermocline case: the power block is switched on too early in the morning and the storage does not manage to supply enough thermal power to drive it at nominal power from 4:30 to 8:30. Moreover, the thermocline reaches quickly the top of the tank. As a result, temperature drops and the power block must work at partial loads.

The 7,5h thermocline shows collection efficiency of 90.9% and discharge efficiency of 70.6%. Hence, overall storage efficiency is just 64.2% (Figure 5). This means that the thermocline supplies only 64.2% of molten salt at the nominal temperature, while the original 7.5h two-tank system was able to supply 100% of molten salt at nominal temperature. However, a portion of the molten salt withdrawn below 545°C is still useful for thermoelectric conversion (highlighted in red at Figure 5) which takes place at partial loads.

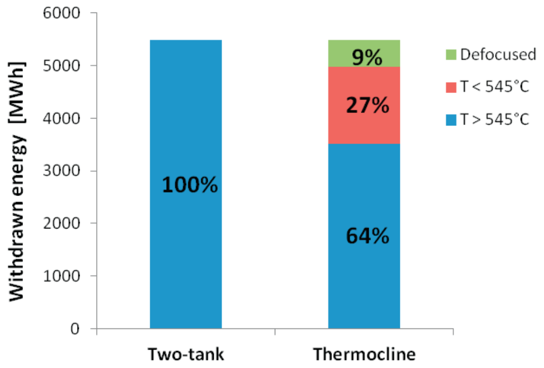

Figure 5: Performance comparison between two-tank storage and thermocline storage

3.3. Optimal thermocline size

It is found that overall efficiency can be improved by changing the storage size. It is known that stratification is improved in tanks with high aspect ratio H/D (height over diameter) [10] [12]. The height of the tank is fixed to 14 meters, which is assessed to be the technical limit for molten salt tanks [2], and the size of the storage is determined by changing the diameter of the vessel.

Interestingly, there is a trade-off between discharge efficiency and collection efficiency. In little tanks, thermocline is very steep, thermal stratification is good and discharge efficiency is high. This is because the vessel is fully charged by hot molten salt and there is no thermal gradient within the tank. When discharge begins, a new steep thermocline is formed in the vessel, which gives high discharge efficiency. Most of withdrawn energy is extracted at temperature above 545°C.

At the same time, little tanks are quickly filled with hot molten salt and many mirrors of the solar field must be defocused soon. So, much energy is wasted and collection efficiency is poor. For example, a little 4h thermocline has a high discharge efficiency of 80.5% but little collection efficiency of 59.7% (Figure 6). As the tank is larger, thermocline is more extended and discharge efficiency decreases. It is interesting to note that for big tanks, such as the 9h or the 11h, collection efficiency is in the range 92-94%. It does not reach 100% because even in those tanks the thermocline occasionally reaches the bottom of the tank during charge process. When this occurs, molten salt leave the tank at temperature above 300°C, some mirrors are placed in stowed position and collection efficiency decreases.

As a result, the 6h tank is the optimal tank size which maximizes the amount of heat withdrawn above 545°C (Figure 6). This thermocline has a collection efficiency of 86.4% and a discharge efficiency of 75.5%. Overall efficiency is 65.2%, which is very close to the 64.2% of the 7.5h vessel.

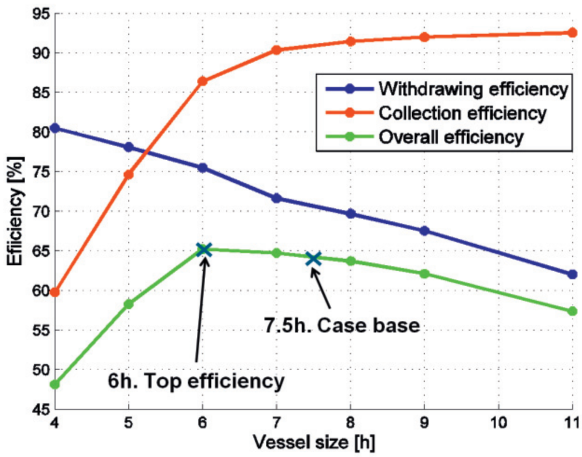

Figure 6: Discharge, collection and storage efficiency depending on thermocline size

Concluding, the two-tank TES system of a CSP plant is replaced with thermocline TES systems. Molten salt mass flow is unchanged and thermocline storage is subjected to the same molten salt mass flow rates of the two-tank system. When considering only molten salt at a temperature above 545°C as useful, optimal thermocline size is between 6h and 7.5h and the thermocline supplies 64-65% of molten salt at a temperature above 545°C. To compare, in a two-tank system 100% of the molten salt are steadily withdrawn at 550 °C.

In brief, thermocline capital investment is about 33% lower than the two-tank one [2], but about 33% of molten salt withdrawn from the thermocline are below the nominal temperature of storing.

3.4. Attempt to improve thermocline efficiency

Tests are performed in order to study possible ways to improve the storage efficiency, always keeping the given plant management and molten salt mass flow rates. Three parameters can be investigated:

- Molten salt type.
- Molten salt and packed bed thermal conductivity.
- Vessel shape factor: tank height versus tank diameter.

Only the effect of shape factor is here reported.

The volume of the vessel is fixed to 6170 m^3, which corresponds to 7.5h Solar Salt thermocline. Storage performance is evaluated changing the shape factor of the vessel. As observed by other authors, tall and thin tanks show better thermal stratification and higher discharge efficiency [2] [5] [10]. This is because thermocline extension is assessed to be averagely 5-7 meters in all tanks; hence the relative portion of tank height occupied by the tank is little in tall tanks.

Tall and thin tanks show an increase in both discharge and collection efficiency. However, it is found efficiency reaches a plateau for vessel taller than 30 meters (Figure 7). Stratification is not much improved for taller vessels, yet heat loss becomes more significant and discharge efficiency decreases. The 30-meters tank has a diameter of 16.2 meters and shows 75.6% of discharge efficiency and 92.0% of collection efficiency; overall efficiency is 69.5%, which is 8.3% (relative) higher than the studied 14 meters case.

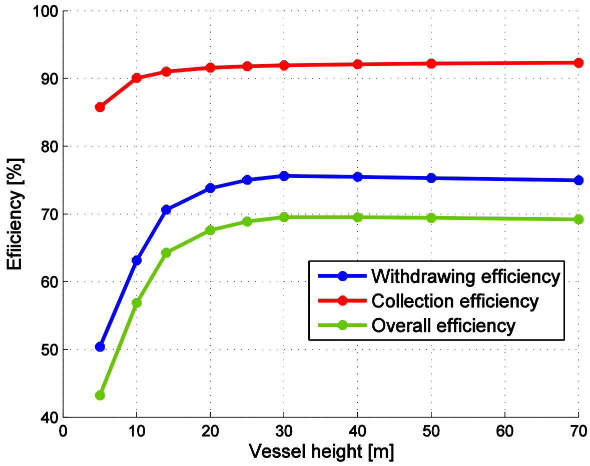

Figure 7: Discharge, collection and overall efficiency versus tank height.

As it is not possible to build 30 meter tall tanks, it is proposed to connect in series two thermocline tanks of 14 meters, to attain a total height of 28 meters. This new configuration is quite attractive but further studies are required. As general remarks, the adoption of two tanks in series would increase the overall surface area (2350 m^2 vs. 1925 m^2 for the single vessel case), with consequent penalties on heat losses. Moreover, costs of the two vessels would be higher because of the two foundations and the higher amount of steel and insulating materials required for the vessel.

4. Conclusions

Thermocline storages have a potential cost reduction of 33% compared to an equal sized state-of-art two-tank storage, however it suffers of lower performances. To deepen eventual penalties, the two-tank storage system of an existing CSP plant is replaced by a thermocline storage system. The management of the plant and the molten salt mass flow rates stored/withdrawn at the storage is optimized for the two-tank system and shows to be not optimized for thermocline storages. It is found that thermocline storage manages to supply only 64% of the stored heat at a temperature above 545°C, versus the 100% of the two-tank system.

It is found that storage efficiency can be improved by changing the size of the vessel. A trade-off between the collection efficiency and discharge efficiency is discovered. Little tanks show a steep thermocline and high discharge efficiency; however, the storage is quickly fully charged and much energy is wasted, leading to low collection efficiency. Larger tanks have larger capacity and high collection efficiency, but the thermocline is more extended and discharge efficiency decreases. As a result, the optimal performance is identified for a thermocline sizing 14-meters tall and between 21.2 – 23.7 meters of diameter, which corresponds to a 6h – 7.5h storage. Still, the storage efficiency is about 33% less compared to the two-tank system. Finally, the effect of the vessel shape factor is analyzed. An increase in height gives advantages until the height of 30 meters because stratification is enhanced, then heat losses become more relevant. As such tall vessels are not feasible, it is suggested to connect in series two thermocline vessels of 14 meters each, to achieve a total height of 28 meters. This innovative configuration is quite attractive but further studies are required.

References

[1] M. Passoni and M. Radice, *Analisi tecnico-economica di sistemi di accumulo per impianti solari termodinamici a concentrazione parabolico-lineare,* Archivio tesi Politecnico di Milano: [https://www.politesi.polimi.it], 2011.

[2] J. Pacheco, S. K. Showalter and W. J. Kolb, "Development of a Molten-Salt Thermocline Thremal Storage System for Parabolic Trough Plants," *Journal of Solar Engineering ,* vol. 124, pp. 123-153, 2002, doi:10.1115/1.1464123.

[3] G. J. Kolb, "Evaluation of Annual Performance of 2-Tank and Thermocline Thermal Storage Systems for Trough Plants," *Journal of Solar Engineering ,* vol. 133, p. doi:10.1115/1.4004239, 2011.

[4] F. Cavallaro, "Fuzzy topsis approach for assessing thermal-energy storage in concentrated solar power systems," *Applied Energy,* vol. 87, pp. 496-503, 2010, doi:10.1016/j.apenergy.2009.07.009.

[5] C. Xu, Z. Wang, Y. He, X. Li and F. Bai, "Sensitivity analysis of the numerical study on the thermal performance of a packed-bed molten salt thermocline thermal storage system," *Applied Energy ,* vol. 92, pp. 65-75, 2012, doi:10.1016/j.apenergy.2011.11.002.

[6] T. E. W. Schumann, "Heat transfer: a liquid flowing through a porous prism," *Journal of the Franklin Institute,* vol. 208, no. 3, pp. 405-416, 1929.

[7] N. Nakao, S. Kaguei and T. Funazkri, "Effect of fluid dispersion coefficient on particle-to-fluid heat transfer coefficients in packed beds: correlation of Nusselt number," *Chemical Engineering Science ,* vol. 34, pp. 325-336, 1979.

[8] N. Wakao and S. Kaguei, Heat and mass transfer in packed beds, New York: Gordon and Beach, 1982.

[9] F. P. Incropera and D. P. D. Witt, Fundamentals of heat and mass transfer, John Wiley & Sons, 2012.

[10] Z. Yang and S. V. Garimella, "Thermal analysis of solar thermal energy storage in a molten-salt thermocline," *Journal of Solar Energy Engineering,* vol. 84, pp. 974-985, 2010, doi:10.1016/j.solener.2010.03.007.

[11] M. Astolfi, M. Binotti, A. Giostri, G. Manzolini, P. Silva, A. DeMarzo and L. Merlo, "Indirect molten salts storage management and size optimization for different solar multiple and sites in a parabolic trough solar power plant," in *SolarPaces*, Granada (Spain), 2011.

[12] X. Yang, X. Yang, J. Ding, Y. Shao, F. Qin and R. Jiang, "Criteria for performance improvement of a molten salt thermocline storage system," *Applied Thermal Engineering ,* vol. 48, pp. 24-31, 2012, doi:10:1016/j.applthermaleng.2012.04.046.